SCIENCE CHINA
Information Sciences

• REVIEW •

July 2026, Vol. 69, Iss. 7, 170402:1–170402:12
https://doi.org/10.1007/s11432-025-4931-2

Special Topic: Advanced Optoelectronics Based on Two-Dimensional Materials

Mechanical modulation of optical properties in 2D materials

Zejuan ZHANG, Shenghai PEI*, Luming WANG, Lijuan YANG, Ming HUANG*, Juan XIA* & Zenghui WANG

Institute of Fundamental and Frontier Sciences, University of Electronic Science and Technology of China, Chengdu 611731, China

Received 20 August 2025/Revised 10 November 2025/Accepted 21 April 2026/Published online 18 June 2026

Abstract Strain engineering, a key enabling strategy for extending Moore's law, employs controlled mechanical modulation to achieve desired modifications in material attributes, such as electrical and optical properties. Thanks to the atomic-level thinness, the optical behaviors of two-dimensional (2D) materials can be remarkably modulated by strain engineering. In this perspective, we highlight two mechanical approaches—tensile strain and compressive strain—and their impact on 2D materials' crystal structure and electronic structure. We also discuss fundamental limitations in strain transfer efficiency and interfacial control, proposing a roadmap for achieving deterministic mechanical-optical modulation and pushing the limit of strain engineering in 2D materials.

Keywords 2D materials, bandgap modulation, phonon dynamics, optical properties, strain engineering

Citation Zhang Z J, Pei S H, Wang L M, et al. Mechanical modulation of optical properties in 2D materials. Sci China Inf Sci, 2026, 69(7): 170402, https://doi.org/10.1007/s11432-025-4931-2

1 Introduction

Strain engineering, leveraging precise mechanical modulation of material properties, has been broadly used in both fundamental research and industrial applications [1, 2]. By strategically introducing lattice mismatch to generate controlled strain, engineers have been able to extend Moore's law into ⩽90 nm nodes [3]. Meanwhile, researchers have successfully overcome the physical limitations of traditional silicon-based field-effect transistors at sub-10 nm technology nodes [4], further extending Moore's law towards the atomic limit.

Thanks to the atomic-level thickness and weak interlayer coupling characteristics, two-dimensional (2D) materials (e.g., transition metal dichalcogenides (TMDCs) and graphene) transcend the physical limitations of conventional 3D materials [5–7], and exhibit highly tunable material properties through strain engineering [8, 9]. In particular, their mechanically tunable optical properties offer important insights into exotic light-matter interactions in these atomically thin crystals [10–19]. Such efforts in the research field leverage multiple inherent advantages of 2D materials (Figure 1): (i) exceptional mechanical flexibility enables lattice modulation via substrate-induced strain, circumventing carrier-mobility degradation and impurity scattering from conventional doping or defect engineering; and (ii) atomic-level cleanliness is preserved in straining processes, allowing efficiently modulation of optoelectronic properties, such as Raman signatures (crystal structure) and photoluminescence (PL)/absorption spectra (electronic band dynamics) [20–35]. Therefore, strain modulation offers a clean methodology for precision property engineering in 2D materials; this atomic-scale control has enabled breakthroughs in ultrasensitive biosensing [36], dynamically reconfigurable metasurfaces [37], and quantum information devices [38].

This perspective aims to provide a brief but structured overview of the distinct advantages of tensile and compressive strain modulation in 2D materials, highlighting recent advances in mechano-optoelectronic characterization. We introduce and categorize strain-engineering strategies, and study their impact on band structure evolution and excitonic responses. We further discuss design principles for strain-programmable photonic devices, fundamental limitations in interfacial strain-transfer efficiency, and possible future directions for this field. We conclude this with an expectation that future research on deterministic control of mechanical-optical coupling will extend the functional boundaries of 2D materials in quantum technologies and adaptive optoelectronics.

* Corresponding author (email: shpei@uestc.edu.cn, huangming@uestc.edu.cn, juanxia@uestc.edu.cn)

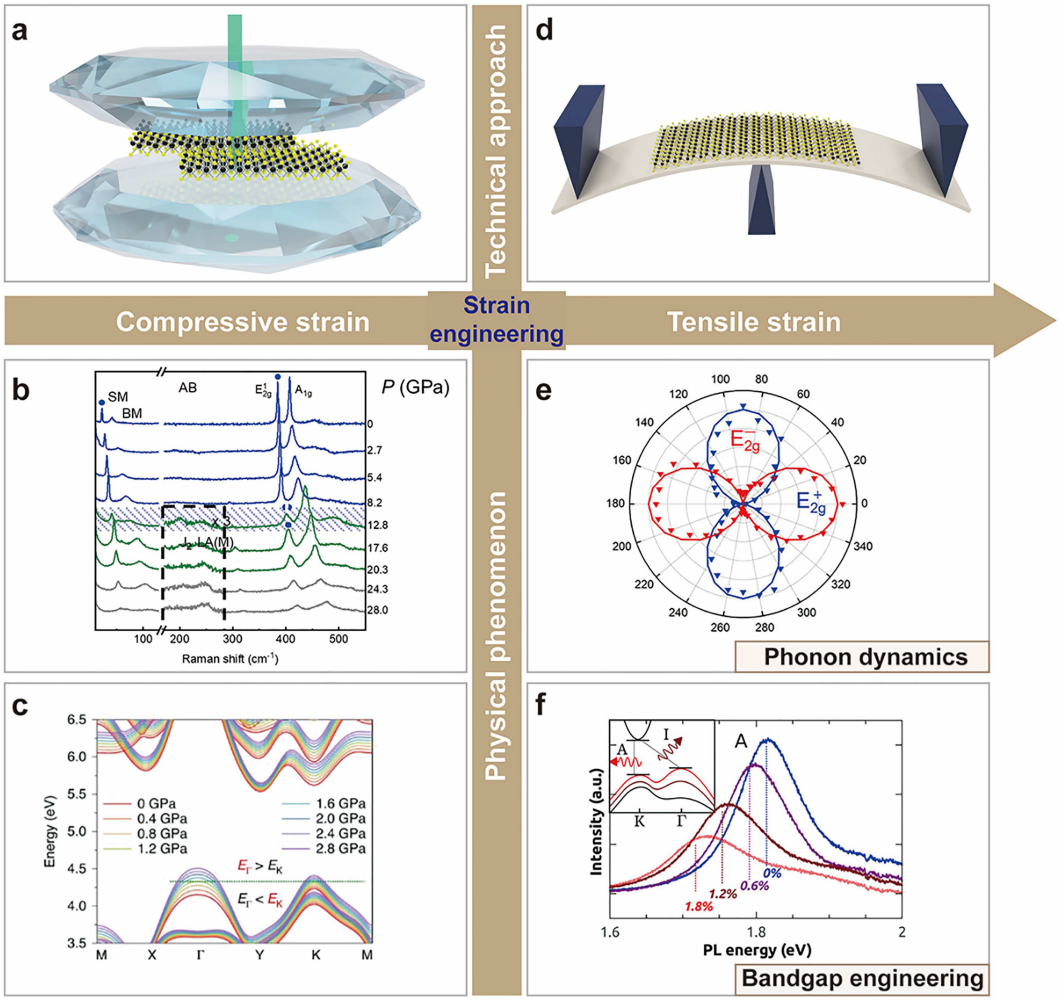

Figure 1 (Color online) Overview of the mechanical modulation of optical properties in 2D materials. Compressive strain driven optical control: diamond anvil cell (DAC) setup for hydrostatic pressure application, enabling reversible lattice variation (especially in *c* axis) in 2D crystals (a), pressure-dependent lattice modulation and phonon dynamics (b), and bandgap engineering (c) [14, 15] Copyright 2024 AIP Publishing, 2021 Springer Nature. Tensile strain modulation: illustration of tensile strain engineering (d), tensile strain induced phonon dynamics (e), and bandgap engineering (f) [17, 18] Copyright 2013 American Chemical Society, 2023 American Chemical Society.

2 Tensile strain: phonon dynamics and bandgap modulation

The application of tensile strain in 2D materials is commonly achieved by deforming the supporting substrate. Standard methods use flexible or pre-patterned substrates [25–28] and bubbles [29–32] where the substrate's deformation induces stretching in the 2D flake. An alternative technique involves direct mechanical manipulation using an atomic force microscope tip [33]. This can tune the material's physical properties by modifying both its lattice structure and electronic structure. By altering the lattice structure, mechanical perturbation exerts a profound influence on phonon dynamics, particularly for in-plane vibrations, typically manifested as bond stretching and symmetry breaking. Further, tensile strain can modify the electronic band structure, enabling precise control over the bandgap. In this section, we classify the fundamental tensile strain that results in the modulation of phonon dynamics and bandgap modulation. Table 1 summarizes the maximum strain values achieved in representative device architectures across various 2D materials, along with the corresponding effects on phonon dynamics and bandgap modulation. Recent advancements in this area are discussed in the following sections with selected examples to highlight key developments.

2.1 Phonon behavior modulated through tensile strain

Phonons are quantized lattice vibrations in crystalline materials, representing collective atomic motions that affect thermal, mechanical, and electronic properties. Tensile strain enables efficient control of phonon dynamics in 2D

Table 1 Representative device architectures, tensile strain types, and maximum strain values for typical materials. The corresponding Raman shift rate or A-exciton shift rate for each work is listed.

Materials	Representative device architectures	Uniaxial/ biaxial strain	Maximum strain rates (%)	Shift rates of E_{2g} modes (cm^{-1}/%) or A exciton (meV/%)	Ref.
1L-MoS_2	Bending the flexible substrate	Uniaxial	5	-1.0 ± 1.0 (E_{2g}^{+}), -4.5 ± 0.3 (E_{2g}^{-})	[18]
2L-MoS_2	Bending the flexible substrate	Uniaxial	5	-1.0 ± 0.9 (E_{2g}^{+}), -4.6 ± 0.4 (E_{2g}^{-})	[18]
1L-MoS_2	Stretching the flexible substrate	Uniaxial	3.6	-0.8 ± 0.1 (E_{2g}^{+}), -2.5 ± 0.3 (E_{2g}^{-})	[28]
1L-MoS_2	Bubble bulge straining	Biaxial	3.5	-2.1 ± 0.2 (E_{2g})	[29]
1L-MoS_2	Stretching the flexible substrate	Uniaxial	0.7	-2.1 (E_{2g})	[35]
2L-MoS_2	Bending the flexible substrate	Uniaxial	1.88	-0.9 ± 0.2 (E_{2g}^{+}), -4.0 ± 0.1 (E_{2g}^{-})	[39]
1L-MoS_2	Bending the flexible substrate	Uniaxial	1.49	-7.4 (E_{2g}^{-})	[40]
1L-MoS_2	Bubble bulge straining	Biaxial	5.6	-5.2 (E_{2g})	[41]
1L & 2L-MoS_2	Bending the flexible substrate	Uniaxial	5	-45 ($A, 1L$), -120 ($A, 2L$)	[18]
1L-MoS_2	Bubble bulge straining	Biaxial	3.5	-41 ± 3 (A)	[29]
1L-MoS_2	Bending the flexible substrate	Uniaxial	1.49	-125 (A)	[40]
1L & 2L-MoS_2	Stretching the flexible substrate	Uniaxial	0.52	-70 ($A, 1L$), -70 ($A, 2L$)	[42]
1L & 2L-MoS_2	Bubble bulge straining	Biaxial	5.6	-99 ± 6 ($A, 1L$), -91 ($A, 2L$)	[41]
2L-MoS_2	Temperature-controlled substrate stretching	Biaxial	0.8	-41 ± 2 (A)	[43]

materials by altering lattice symmetry and deforming atomic bonds. The underlying mechanism is the stress-induced modification of interatomic force constants and vibrational phases (between adjacent atoms), which could significantly alter phonon dispersion, lift mode degeneracy, and modulate electron–phonon coupling (EPC) strength. Raman spectroscopy—by tracking frequency shifts, peak broadening, and the appearance or disappearance of specific modes—serves as a powerful, noninvasive probe to quantify the strain-induced changes in phonon behaviors.

On the application of tensile strain, bonds in 2D materials can elongate, reducing the bond stiffness and causing phonon softening (frequency redshift). For instance, the G peak of graphene is found to redshift at a rate of $\sim$5 cm^{-1}/% (per percent strain) under uniaxial tensile strain [26]. In addition, symmetry breaking can also happen under uniaxial strain, which often lifts the degeneracy of certain in-plane modes, splitting one Raman peak into two peaks (corresponding to two similar modes vibrating in orthogonal directions). For instance, the G peak of graphene separates into G^+ and G^- peaks. As another example, the doubly degenerate E_{2g} phonons of MoS_2 also split when tensile strain is applied (Figure 2), while the peak position of the out-of-plane A_{1g} mode remains nearly unchanged, as the out-of-plane vibrations are much less sensitive to in-plane tensile strain [28, 39, 40]. It is worth noting that the tensile-strain-induced shifts of Raman peaks can depend on the relative angle between the applied uniaxial strain and the crystal orientation, which is particularly pronounced in anisotropic 2D materials such as ReS_2 [44, 45].

2.2 Bandgap modulation induced by tensile strain

The bandgap of 2D materials is highly sensitive to structural deformation, and tensile strain can serve as a powerful modulation tool through directly altering interatomic bond lengths and bond angles (Figure 3(a)) [17–56]. For example, tensile-strain-induced direct-bandgap redshift at a rate of $\sim$70 meV/% applied strain in monolayer MoS_2 has been successfully observed in PL spectroscopy, as shown in Figure 3(b) [17]. Such strain-driven indirect-to-direct gap transitions are also found in many other 2D materials, including both isotropic (graphene [25–27], TMDCs [41–43, 46–57]) and anisotropic ones (ReS_2 [58, 59], and black phosphorus [60–62]).

Moreover, the modulation of the bandgap induced by tensile strain can depend on the layer number of 2D materials [17, 60, 61], offering an interesting viewpoint for the interplay between the strain and layer degrees of freedom. Figure 3(c) illustrates the evolution of the band structure of black phosphorus with varying layer numbers under both uniaxial and biaxial strains as revealed by infrared absorption spectroscopy. The band-shift rate increases with the number of layers, from 158 meV/% for 3L to 185 meV/% for 4L, demonstrating a clear layer-number dependence [60, 61].

Tensile strain engineering provides a versatile approach for tuning and tailoring the optical properties of 2D materials, which can play a unique role in the exploration and development of tunable 2D optical and optoelectronic devices. The layer-dependent responses and material-specific behaviors further offer rich opportunities for engineering material properties in combination with the controlled application of tensile strain.

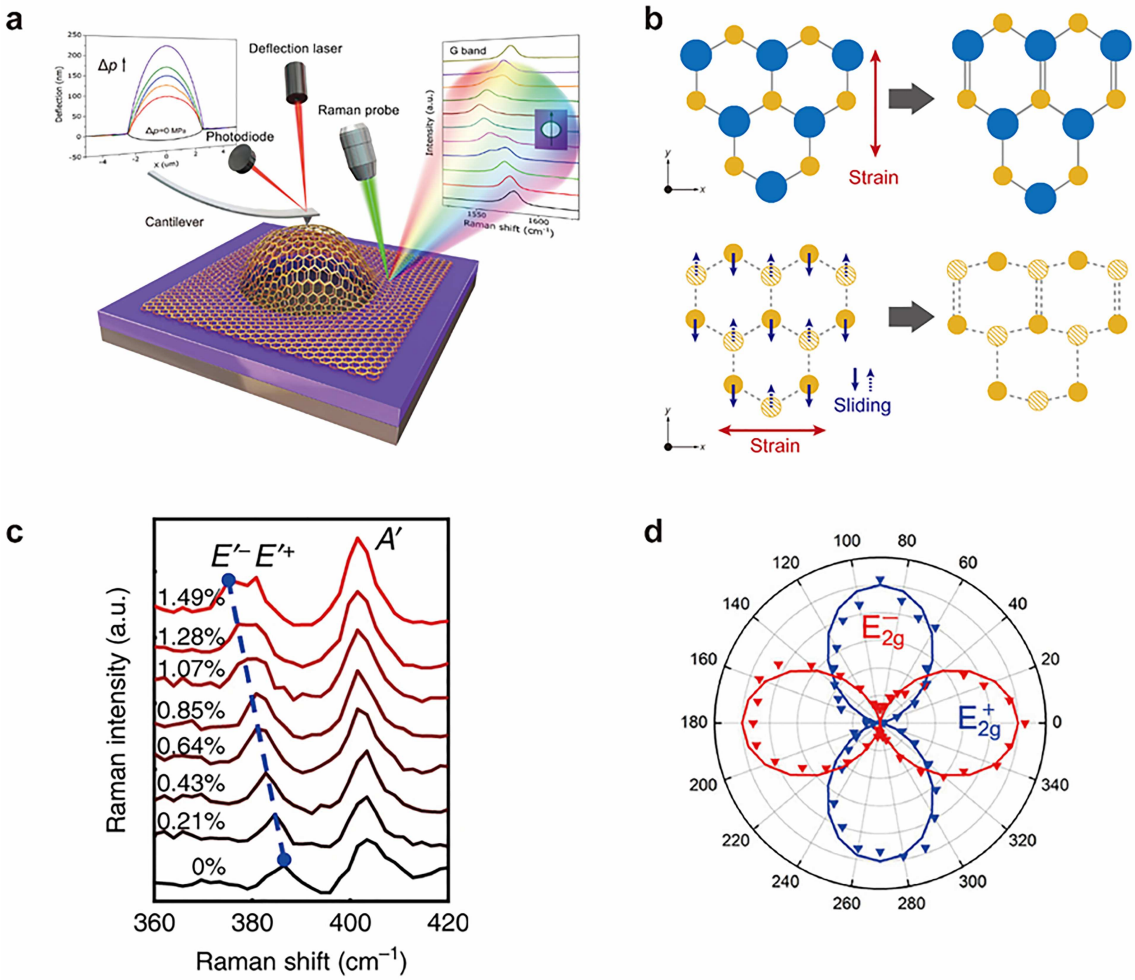

Figure 2 (Color online) Strain-induced phonon softening and splitting in 2D materials. (a) Evolution of the Raman spectra of the G bands of graphene under strain [31] Copyright 2017 American Physical Society. (b) Lattice structure of bilayer MoS_2 under uniaxial strain [39] Copyright 2017 Nature Publishing Group. (c) Evolution of the Raman spectra of the E_{2g} bands of monolayer MoS_2 under strain. The E_{2g} peak splits into E_{2g}^+ and E_{2g}^- due to the breaking of crystal symmetry [40] Copyright 2020 Nature Publishing Group. (d) Polarized Raman spectrum of in-plane intralayer modes E_{2g}^+ and E_{2g}^-, which can determine the direction of strain with respect to the crystal orientation [19] Copyright 2023 American Chemical Society.

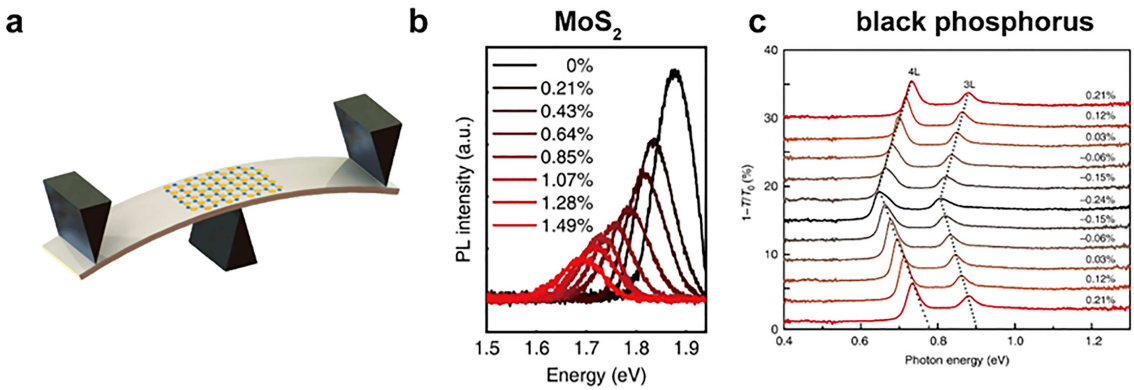

Figure 3 (Color online) Strain induced bandgap shifting in 2D materials. (a) The three-point bending apparatus. Note that the 2D material flake is in the μm range. (b) Strain induced direct to indirect band gap transition in MoS_2 [40] Copyright 2020 Nature Publishing Group. (c) Infrared absorption spectroscopy spectra for the black phosphors with different layer numbers [61] Copyright 2019 Nature Publishing Group.

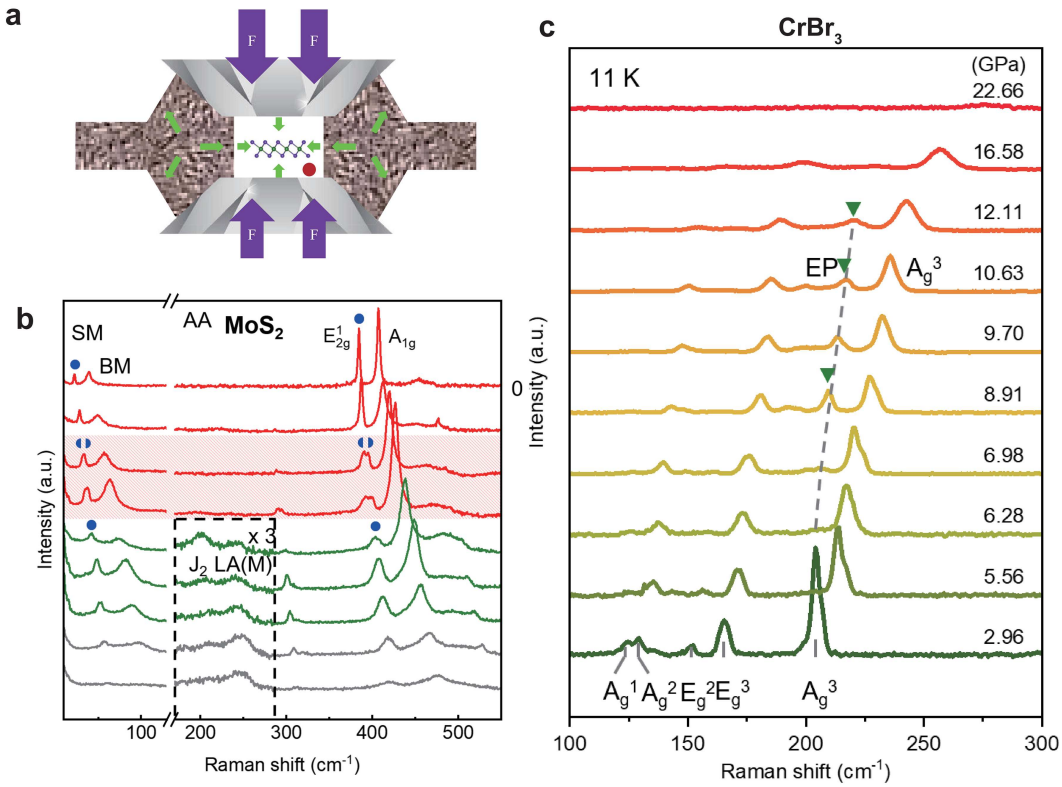

Figure 4 (Color online) Pressure induced phonon hardening and phase transition in 2D materials. (a) Schematic illustration of phonon dynamics and phase transition in 2D material by using hydrostatic pressure through a DAC. (b) Raman spectra upon pressurization (0–28.0 GPa) for bilayer MoS_2 [14] Copyright 2024 AIP Publishing. (c) Pressure enhanced EPC in $CrBr_3$ [64] Copyright 2024 IOP Publishing.

3 Compressive strain: phase transitions and bandgap engineering

While tensile strain predominantly modifies the intralayer atomic structure of 2D materials, compressive strain, in contrast, can engender both intralayer and (more remarkably) interlayer deformation. This enables unique control of physical properties, including bandgap engineering, tuning of charge-carrier concentration/mobility, and modulation of EPC strength. Currently, the DAC is the primary and most widely used method for applying compressive strain in 2D materials research. A schematic of a typical DAC is shown in Figure 4(a). This technique enables precise control of hydrostatic stress environments exceeding 400 GPa—a regime comparable to Earth's core conditions—thereby facilitating unprecedented investigations into extreme-pressure phenomena in such atomically thin condensed matter systems. DAC anvils feature a range of culet sizes, such as 200, 400, and 600 μm. In general, the smaller the culet size, the higher the achievable pressure. In most cases, while studying 2D materials, the applicable pressure range typically remains below 30 GPa; therefore, 400 μm (or similar) culet size is predominantly used [63].

The continuous and reversible microscopic changes in 2D materials induced by pressure offer unparalleled advantages in tuning efficiency and controllability for exploring material properties. Unsurprisingly, pressure engineering via DAC has become an important technology for studying structural and electronic phase transitions in 2D materials, which can further be leveraged to explore highly sensitive pressure sensors and adaptive optoelectronic devices in which dynamic control over optical characteristics is desirable. In this section, we categorize the fundamental compressive strain achieved via DAC that results in the tuning of phonon dynamics and bandgap behavior. Table 2 summarizes the maximum achievable compressive strain values for various materials, along with the corresponding Raman shift or bandgap behavior.

3.1 Phonon dynamics and phase transition tuned by compressive strain

Pressure can effectively induce structural/electronic phase transitions and tune interlayer coupling, which are often manifested in phonon behaviors in 2D materials [86]. Raman spectroscopy is widely used in probing phonon dynamics; thus, it is often used for studying material properties under pressure engineering, elucidating phase transitions through features such as pressure-induced shifts and broadening of Raman peaks [66–68, 87–90]. For instance, pressure can stiffen in-plane phonon modes and enhance interlayer vibrations, triggering semiconductor-

Table 2 Compressive strain limits and resulting spectral responses in typical materials.

Materials	Maximum pressure (GPa)	Maximum shift Raman modes (cm^{-1})	Bandgap behavior	Refs.
2L MoS_2	30.40	78.47 (2H phase), 72.92 (3R phase)	Bandgap changeover	[14, 65]
WSSe	31.60	66	Bandgap closure beyond 30.0 GPa	[20]
Fe_3GeTe_2	20.00	11	–	[22]
MoS_2/WS_2	8	26.4	Direct to indirect transition	[23]
ReS_2 bulk	30.24	65	Indirect bandgap to direct	[66]
1–3L black phosphorus	15	1L: 52, 2L: 50, 3L: 30	–	[67]
MoS_2 (powder)	57.00	130	–	[68]
2L-WS_2	25.00	68.41 (2H), 68.36 (3R)	Bandgap closure	[69]
Twisted 2L-WSe_2	6.95	11.15	Bandgap changeover	[70]
1T-$HfSe_2$	40	80	Bandgap closure	[71]
1L-MoS_2 (2H and 1T′)	30.7	79.82 (2H), 76.75 (1T′)	Direct to indirect transition (2H)	[72]
1L-MoS_2 and 1L-WSe_2	4.50	32.50 1L-MoS_2, 20.00 1L-WSe_2	Direct to indirect transition	[65, 73]
hBN/WS_2/hBN	14.1	40	Direct to indirect transition	[74]
$CrBr_3$	22.66	82.00	–	[64]
WTe_2 bulk	17.9	40.00	–	[75]
1L-$MoTe_2$ (1T′)	34.9	65.00	–	[76]
$MoSe_2$	50.00	80.00	Bandgap closure at ∼40 GPa	[77]
7L-graphene	51.70	200.00	–	[78]
1–2L graphene	22.00	70	–	[79–81]
3L graphene	51.5	15 (at 3 GPa)	Bandgap opening above ∼30.1 GPa	[79, 80, 82]
Graphite	14.00	45	–	[83]
Graphene nanoplates	30.44	100	–	[84]
h-BN	10.00	50	–	[85]

to-metal transitions [69–72]. One such example is shown in Figure 4(b): in bilayer MoS_2 with different stacking configurations, a pressure-driven semiconductor-to-metal transition (from the 2H to 1T′ phase) is accompanied by pronounced shifts and broadening of the A_{1g} and E_{2g} Raman modes [72, 73].

Pressure engineering can also significantly enhance EPC in 2D materials [64, 74, 91]. As shown in Figure 4(c), a characteristic vibrational mode (EPC mode) and periodic Raman patterns emerge above 6.28 GPa, yielding a clear ∼40% increase in EPC for layered $CrBr_3$ [64].

3.2 Electronic bandgap modulation driven by compressive strain

By compressing the lattice, pressure shortens interatomic distances, strengthens orbital overlaps, and enhances EPC, thereby reshaping band structures and triggering semiconductor-to-metal transitions. For example, in semiconducting 2D materials such as TMDCs, pressure narrows bandgap via increased interlayer coupling and modified valence/conduction band edges, which is often accompanied by structural phase changes [64, 69–77, 91, 92]. As an example, Figures 5(b) and (c) illustrate such an effect in a $WSe_2/MoSe_2$ heterostructure, where pressure tunes interlayer coupling and induces a clear band changeover [15].

Moreover, in zero-gap 2D materials such as graphene, pressure induces interlayer hybridization that breaks inversion symmetry and opens a tunable bandgap [78–84], with reported values ranging from 100 meV in monolayer graphene [79] to 2.5 ± 0.3 eV in trilayer graphene [82]. In contrast, wide-gap 2D materials like hBN show exceptional electronic stability under pressure, making an ideal substrate or insulating layer for high-pressure device integration [85, 93–95].

Collectively, these studies establish pressure engineering as a powerful approach for tailoring the optical properties of 2D materials. With the capability of triggering pressure-driven structural/electronic phase transitions and finely tuning interlayer coupling, the approach paves the way for ultrasensitive pressure sensors and adaptive optoelectronic devices, opening vast design space for on-demand property control via precise compression.

4 Summary and outlook

In this mini review, we have discussed the effects of tensile and compressive strain on the optical properties of 2D materials. Here we present a simple but quantitative comparison for different types of 2D materials by using the

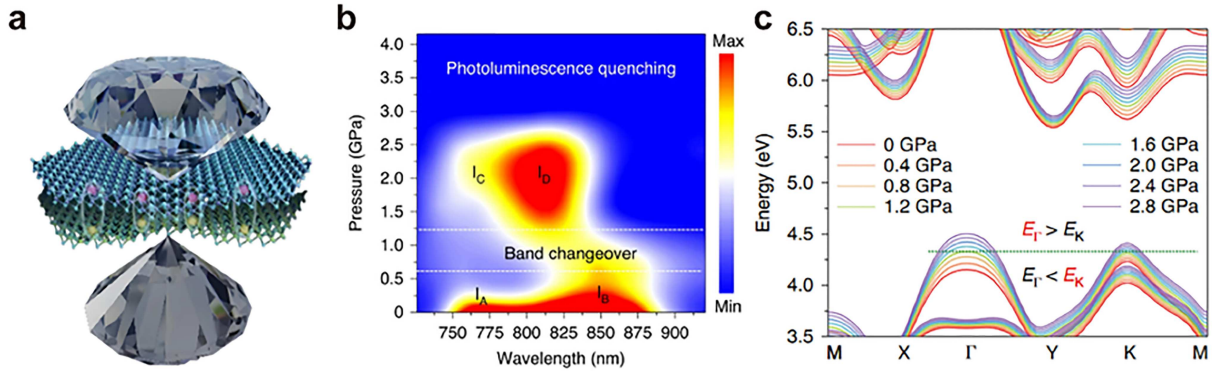

Figure 5 (Color online) Pressure induced bang changeover in 2D materials. (a) Schematic illustration of band engineering in 2D material by using hydrostatic pressure through a DAC. (b) Pressure induced bang changeover in WSe_2–$MoSe_2$ van der Waals heterostructure. (c) Band changeover of VBM from K to Γ [15] Copyright 2021 Springer Nature.

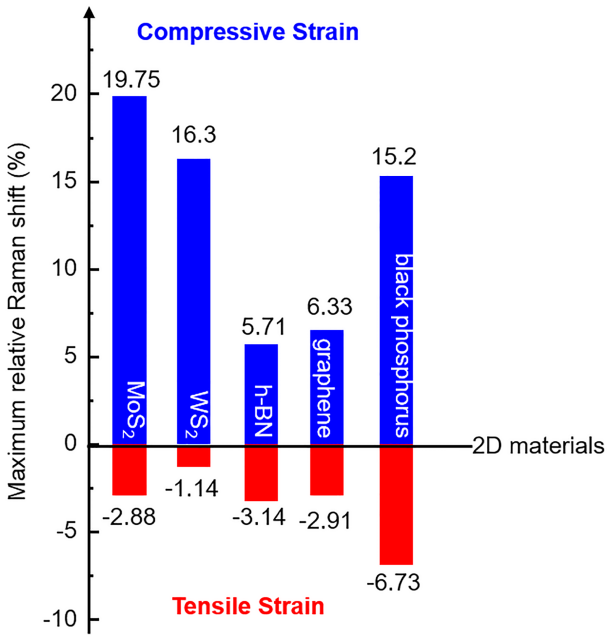

Figure 6 (Color online) A comparative summary of the reported maximum relative Raman shift (μ) values for typical 2D materials under tensile and compressive strain, with data sourced from: MoS_2 [40, 72], WS_2 [57, 69], h-BN [46, 85], graphene [27, 79] and BP [62, 67].

maximum relative Raman shift $\mu = \Delta\omega/\omega_0$, where $\Delta\omega$ is the Raman shift induced by tensile/compressive strain and ω_0 is the initial frequency of the specific Raman peaks in the unstrained 2D materials. We calculate these values from literature for several representative 2D materials—including MoS_2 [40, 72], WS_2 [57, 69], h-BN [46, 85], graphene [27, 79] and BP [62, 67]—under both tensile and compressive strain. The results are summarized in Figure 6. It is particularly noteworthy that the attainable strain ranges for tensile and compressive loading differ significantly. Although tensile strain can be applied in both uniaxial and biaxial ways in the atomic plane, it is ultimately limited by material fracture, with a finite applicable range.

In contrast, compressive strain that helps reduce interlayer distances and even in-plane bond lengths can generally be applied to a much greater extent. Nevertheless, compressive strain is generally applied in a hydrostatic way (which means the compression is applied in all directions) rather than in-plane (which would require suppression of out-of-plane buckling, which would be technically difficult). The unique advantages of tensile and compressive strain in 2D materials—such as continuous tunability, reversibility, and site-specific modulation—further strengthen the potential of this approach, offering pathways to tailor material properties with a precision unattainable by purely electrical or chemical means. Although there are challenges in scalability and integration, recent experimental advances underscore the field's viability and illuminate compelling opportunities for future breakthroughs in flexible optoelectronics and on-demand photonic devices.

5 Challenges and future perspectives

5.1 Challenges

As outlined previously, 2D materials exhibit exceptional responsiveness to strain, enabling precise engineering of optoelectronic properties through both tensile strain and compressive strain. Although these mechanical modulation strategies have achieved remarkable success in optically active lattice manipulation, there remain some important limitations. This subsection examines some of the key challenges.

• **Strain-transfer loss.** In strain-engineering studies of 2D materials, the induced strain is generally estimated from quantitative analysis of substrate deformation. However, strain-transfer loss—critically dependent on interfacial adhesion and substrate mechanical properties such as stiffness or Young's modulus—has remained as a ubiquitous challenge in virtually all strain-modulated systems [96, 97]. Therefore, it is important to note that the maximum strain limit achievable experimentally is not just limited by the method used, but also (and likely more) limited by the strain transfer efficiency between the 2D material and its substrate.

During straining of the substrate, interfacial sliding and delamination frequently induce localized relaxation, which can even relax the 2D flake toward near-zero residual strain via elastic recovery. For instance, in strain experiments with MoS_2, the strain-transfer efficiency dramatically increases with the Young's modulus of the substrates [98, 99]. A soft substrate like Polydimethylsiloxane (PDMS) ($\sim$500 kPa) has mere $\sim$1% efficiency, but using a stiffer polypropylene ($\sim$1.5 GPa) substrate raises this efficiency to $\sim$75%. With even higher-modulus substrates, the efficiency can reach $\sim$90%, transferring 4.7% strain to the MoS_2 layer from an applied 5% strain. These findings unequivocally establish the substrate's Young's modulus as the key determinant of the strain-transfer efficiency and indicate that a modulus significantly greater than 500 MPa is essential for highly effective strain transfer. Therefore, to achieve higher strain in such experiments, the strain-transfer challenge must be properly addressed.

To overcome this limitation, it is essential to first establish a clear understanding of the strain transfer mechanism. This understanding necessitates the development of standardized measurement methodologies and systematic research to specifically quantify the impact of interfacial adhesion on strain transfer efficiency. Furthermore, improved methods for clamping, adhesion, and strain application are required to mitigate interfacial sliding, thereby significantly enhancing both the efficiency and reliability of strain transfer. Through advanced mechanical design and interfacial engineering, we anticipate that 2D materials can be strained in a more controlled and accessible manner—potentially reaching their intrinsic fracture limit [98]—while simultaneously facilitating optical measurements.

• **Unexplored high-pressure phase diagrams.** Under compression, materials often adopt complex metastable structures with novel physical properties. However, predicting the formation mechanisms, stability, and physicochemical characteristics has remained largely elusive for 2D materials. This situation stems from two critical limitations. First, most first-principles methods (such as density-functional theory, DFT) suffer from reduced accuracy at extreme pressures, due to electron correlation and other intricate quantum behaviors that emerge under extreme conditions. Second, the scarcity of reliable high-pressure phase diagrams deprives experimentalists of reliable theoretical guidance, leaving researchers largely relying on empirical exploration. The absence of robust models and comprehensive data introduces profound uncertainty, hampering systematic understanding of material properties under extreme compression.

5.2 Future perspectives

Notwithstanding these challenges, substantial research opportunities emerge through the development of advanced experimental methodologies. We hereby propose several promising directions to address both limitations (Figure 7).

• **Synergy between strain and electric field.** The synergistic application of uniaxial tensile strain and electric field presents a novel paradigm for modulating material properties, yet its practical application in wearable devices still requires addressing a tradeoff between the high stiffness required for efficient strain transfer and the flexibility essential for wearing comfort. Studies clearly demonstrate the correlation between strain-transfer efficiency and substrate stiffness. Emerging approaches included structured substrate designs such as Ferris wheel-shaped island structures [99] and conformable phased arrays [100], and copolymer substrate materials [101], which offer effective pathways to resolve this. These innovative designs maintain sufficient local stiffness to enhance strain-transfer efficiency while ensuring that the overall structure meets the flexibility requirements of wearable applications. Electric field regulation serves as a complementary strategy for engineering the optoelectronic properties of 2D materials [102]. Furthermore, the flexoelectric effect—where a strain gradient induces polarization in otherwise nonpolar materials—can enable additional coupling between mechanical deformation and electrical response [103]. This integrated methodology can not only clarify the interaction between strain and electric field, but also provide

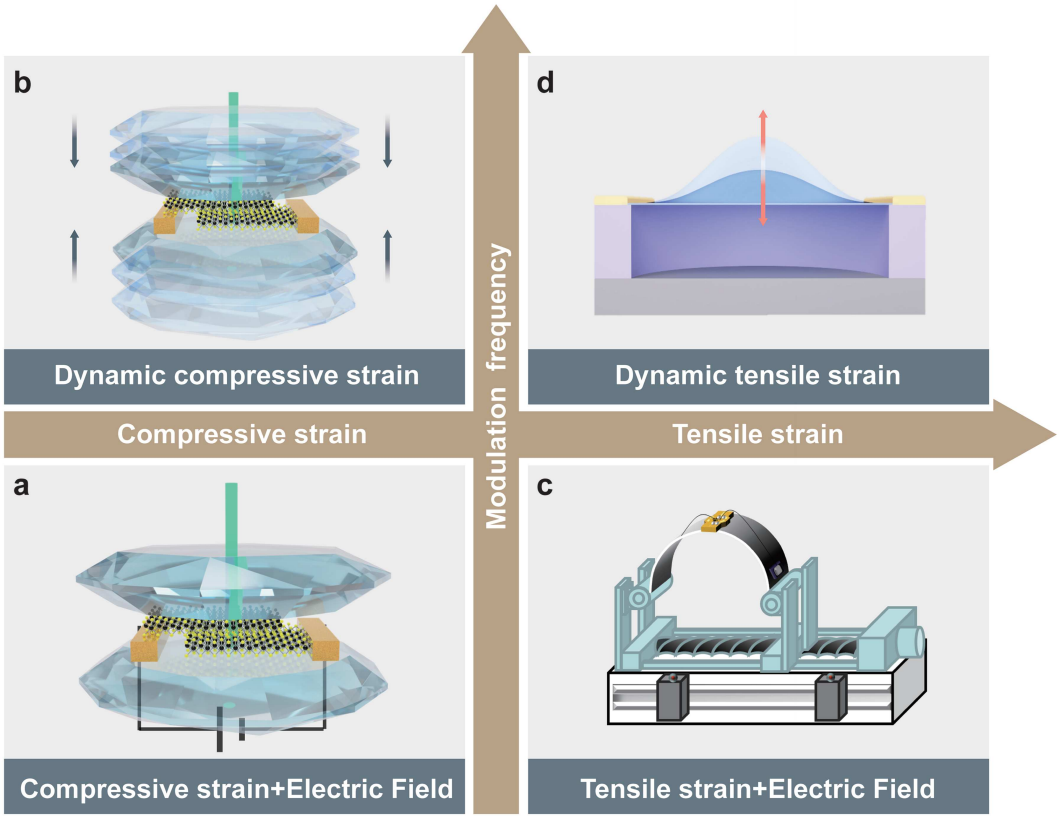

Figure 7 (Color online) Potential experimental techniques combining multiple fields together. (a) Pressure and electric field; (b) rapid compression strain engineering; (c) strain and electric field; (d) dynamic strain engineering.

useful insights for optimizing flexible piezotronic devices. In addition, in situ electrical characterization during strain–stress cycle could be useful for validating operational durability of 2D materials in flexible and stretchable sensors [104–107].

• **Dynamic tensile strain engineering.** Dynamic tensile strain engineering, typically enabled by driving suspended 2D material into mechanical resonance, overcomes the inherent physical limitations of static modulation by employing high-frequency cyclic deformation. This approach can avoid interface-defect generation caused by atomic slippage while achieving enhanced strain manipulation efficiency via resonant amplification effects [108–114]. Furthermore, the intrinsic cross-frequency coupling in dynamic strain might synchronously enhance EPC. Nevertheless, significant knowledge gaps exist in understanding optical property modulation under high-frequency dynamic strain (>10 MHz), especially regarding time-resolved phonon-bottleneck effects during strain cycling [115].

• **Combination of pressure and electric field.** Under pressure, the interlayer electric field can further modulate optical properties—most notably by enhancing interlayer charge transfer and strengthening interlayer exciton behavior. Electrical transport measurements performed under extreme pressures (1–10 GPa range) are therefore essential for validating the performance of ultrahigh-pressure sensors based on 2D materials. In addition, the possibility of gate tuning under high pressure offers a new possibility to study and tune material properties in 2D crystals. We expect that investigating gate-controlled interlayer exciton behavior under precisely regulated pressure conditions will become feasible in the near future, representing a natural progression toward more sophisticated studies in this field.

• **Technique for applying rapid compression.** Millisecond-scale rapid compression, combined with in situ synchrotron Raman spectroscopy, can capture transient states that are inaccessible to conventional pseudo-static pressurizing. It can thus resolve phase-transition pathways and atomic-scale dynamics of pressure-induced phase transitions [116–118]. The rapid compression technique, therefore, offers a potentially transformative approach for discovering novel phases and probing nonequilibrium dynamics in 2D materials.

Acknowledgements This work was supported by National Natural Science Foundation of China (Grant Nos. T2325007, 62450003, 12574035, 62104029, 52373223), Open Project of State Key Laboratory of High Pressure and Superhard Materials (Jilin University) (Grant No. 202506), Opening Project of State Key Laboratory of Metastable Materials Science and Technology (Yanshan University) (Grant No. 202504), and Sichuan Provincial Natural Science Foundation for Distinguished Young Scholars (Grant No. 25NSFJQ0277).

References

1 Yu D, Feng J, Hone J. Elastically strained nanowires and atomic sheets. MRS Bull, 2014, 39: 157–162
2 Li J, Shan Z, Ma E. Elastic strain engineering for unprecedented materials properties. MRS Bull, 2014, 39: 108–114
3 Thompson S E, Parthasarathy S. Moore's law: the future of Si microelectronics. Mater Today, 2006, 9: 20–25
4 Ieong M, Doris B, Kedzierski J, et al. Silicon device scaling to the sub-10-nm regime. Science, 2004, 306: 2057–2060
5 Carey T, Cassidy O, Synnatschke K, et al. High-mobility flexible transistors with low-temperature solution-processed tungsten dichalcogenides. ACS Nano, 2023, 17: 2912–2922
6 Ricciardulli A G, Yang S, Smet J H, et al. Emerging perovskite monolayers. Nat Mater, 2021, 20: 1325–1336
7 Yang S, Zhang P, Nia A S, et al. Exfoliation and engineering of 2D materials through electrochemistry. CCS Chem, 2024, 6: 2368–2391
8 Wang M, Huang M, Luo D, et al. Single-crystal, large-area, fold-free monolayer graphene. Nature, 2021, 596: 519–524
9 Huang M, Bakharev P V, Wang Z J, et al. Large-area single-crystal AB-bilayer and ABA-trilayer graphene grown on a Cu/Ni(111) foil. Nat Nanotechnol, 2020, 15: 289–295
10 Pimenta Martins L G, Ruiz-Tijerina D A, Occhialini C A, et al. Pressure tuning of minibands in MoS_2/WSe_2 heterostructures revealed by moiré phonons. Nat Nanotechnol, 2023, 18: 1147–1153
11 Zhu M, Zhang Z, Zhang T, et al. Exchange between interlayer and intralayer exciton in WSe_2/WS_2 heterostructure by interlayer coupling engineering. Nano Lett, 2022, 22: 4528–4534
12 Huang Z, Bai Y, Zhao Y, et al. Observation of phonon Stark effect. Nat Commun, 2024, 15: 4586
13 Lv P, Zhao D, Ma Z, et al. Pressure-modulated interface engineering toward realizing Core@Shell configuration transition. Nano Lett, 2023, 23: 11982–11988
14 Jiao C, Pei S, Zhang Z, et al. Exploration toward a new stacking-pressure phase diagram in bilayer AA- and AB-MoS_2. Appl Phys Rev, 2024, 11: 031417
15 Xia J, Yan J, Wang Z, et al. Strong coupling and pressure engineering in WSe_2-$MoSe_2$ heterobilayers. Nat Phys, 2021, 17: 92–98
16 Zhu C R, Wang G, Liu B L, et al. Strain tuning of optical emission energy and polarization in monolayer and bilayer MoS_2. Phys Rev B, 2013, 88: 121301
17 Conley H J, Wang B, Ziegler J I, et al. Bandgap engineering of strained monolayer and bilayer MoS_2. Nano Lett, 2013, 13: 3626–3630
18 Quan J, Chen G, Linhart L, et al. Quantifying strain in Moiré superlattice. Nano Lett, 2023, 23: 11510–11516
19 Jiao C, Pei S, Wu S, et al. Tuning and exploiting interlayer coupling in two-dimensional van der Waals heterostructures. Rep Prog Phys, 2023, 86: 114503
20 Hong M, Dai L, Hu H, et al. Pressure-driven structural and electronic transitions in a two-dimensional Janus WSSe Crystal. Inorg Chem, 2023, 62: 16782–16793
21 Gao Y, Xu Q, Farooq M U, et al. Switching the Moiré lattice models in the twisted bilayer WSe_2 by strain or pressure. Nano Lett, 2023, 23: 7921–7926
22 Dang N, Kozlenko D P, Lis O N, et al. High pressure-driven magnetic disorder and structural transformation in Fe_3GeTe_2: emergence of a magnetic quantum critical point. Adv Sci, 2023, 10: 2206842
23 Kim J S, Maity N, Kim M, et al. Strain-modulated interlayer charge and energy transfers in MoS_2/WS_2 heterobilayer. ACS Appl Mater Interfaces, 2022, 14: 46841–46849
24 Yin S, Luo Q, Wei D, et al. Strain and external electric field modulation of the electronic and optical properties of GaN/WSe_2 vdWHs. Phys E-Low-Dimensional Syst NanoStruct, 2022, 142: 115258
25 Peng Z, Chen X, Fan Y, et al. Strain engineering of 2D semiconductors and graphene: from strain fields to band-structure tuning and photonic applications. Light Sci Appl, 2020, 9: 190
26 Huang M, Yan H, Chen C, et al. Phonon softening and crystallographic orientation of strained graphene studied by Raman spectroscopy. Proc Natl Acad Sci USA, 2009, 106: 7304–7308
27 Yoon D, Son Y W, Cheong H. Strain-dependent splitting of the double-resonance Raman scattering band in graphene. Phys Rev Lett, 2011, 106: 155502
28 Wang Y, Cong C, Qiu C, et al. Raman spectroscopy study of lattice vibration and crystallographic orientation of monolayer MoS_2 under uniaxial strain. Small, 2013, 9: 2857–2861
29 Yang R, Lee J, Ghosh S, et al. Tuning optical signatures of single- and few-layer MoS_2 by blown-bubble bulge straining up to fracture. Nano Lett, 2017, 17: 4568–4575
30 Huang Y, Wang X, Zhang X, et al. Raman spectral band oscillations in large graphene bubbles. Phys Rev Lett, 2018, 120: 186104
31 Wang G, Dai Z, Wang Y, et al. Measuring interlayer shear stress in bilayer graphene. Phys Rev Lett, 2017, 119: 036101
32 Guo Y, Li B, Huang Y, et al. Direct bandgap engineering with local biaxial strain in few-layer MoS_2 bubbles. Nano Res, 2020, 13: 2072–2078
33 Manzeli S, Allain A, Ghadimi A, et al. Piezoresistivity and strain-induced band gap tuning in atomically thin MoS_2. Nano Lett, 2015, 15: 5330–5335
34 Scalise E, Houssa M, Pourtois G, et al. Strain-induced semiconductor to metal transition in the two-dimensional honeycomb structure of MoS_2. Nano Res, 2012, 5: 43–48
35 Rice C, Young R J, Zan R, et al. Raman-scattering measurements and first-principles calculations of strain-induced phonon shifts in monolayer MoS_2. Phys Rev B, 2013, 87: 081307
36 Loan P T K, Zhang W, Lin C, et al. Graphene/MoS_2 heterostructures for ultrasensitive detection of DNA hybridisation. Adv Mater, 2014, 26: 4838–4844
37 Li M Y, Chen C H, Shi Y, et al. Heterostructures based on two-dimensional layered materials and their potential applications. Mater Today, 2016, 19: 322–335
38 Tang H, Wang Y, Ni X, et al. On-chip multi-degree-of-freedom control of two-dimensional materials. Nature, 2024, 632: 1038–1044
39 Lee J U, Woo S, Park J, et al. Strain-shear coupling in bilayer MoS_2. Nat Commun, 2017, 8: 1370
40 Li Z, Lv Y, Ren L, et al. Efficient strain modulation of 2D materials via polymer encapsulation. Nat Commun, 2020, 11: 1151
41 Soriano D, Marian D, Dubey P, et al. Strain-induced valley transport in a $CrBr_3WSe_2CrBr_3$ van der Waals heterostructure. Phys Rev B, 2024, 109: 115434
42 He K, Poole C, Mak K F, et al. Experimental demonstration of continuous electronic structure tuning via strain in atomically thin MoS_2. Nano Lett, 2013, 13: 2931–2936
43 Carrascoso F, Lin D Y, Frisenda R, et al. Biaxial strain tuning of interlayer excitons in bilayer MoS_2. J Phys Mater, 2020, 3: 015003
44 Zhou Z H, Wei B C, He C Y, et al. Anisotropic Raman scattering and mobility in monolayer $1T_d$-ReS_2 controlled by strain engineering. Appl Surf Sci, 2017, 404: 276–281
45 Niehues I, Deilmann T, Kutrowska-Girzycka J, et al. Uniaxial strain tuning of Raman spectra of a ReS_2 monolayer. Phys Rev B, 2022, 105: 205432
46 Androulidakis Ch, Koukaras E N, Poss M, et al. Strained hexagonal boron nitride: phonon shift and Grüneisen parameter. Phys Rev B, 2018, 97: 241414
47 Zhang D, Ge C, Wang Y, et al. Enhancing layer-engineered interlayer exciton emission and valley polarization in van der Waals heterostructures via strain. ACS Nano, 2024, 18: 17672–17680
48 Qi Y, Sadi M A, Hu D, et al. Recent progress in strain engineering on van der Waals 2D materials: tunable electrical, electrochemical, magnetic, and optical properties. Adv Mater, 2023, 35: 2205714
49 Liu N, Wang C, Zhang Y, et al. Intralayer strain tuned interlayer magnetism in bilayer CrSBr. Phys Rev B, 2024, 109: 214422
50 Ripin A, Peng R, Zhang X, et al. Tunable phononic coupling in excitonic quantum emitters. Nat Nanotechnol, 2023, 18: 1020–1026

51 Lloyd D, Liu X, Christopher J W, et al. Band gap engineering with ultralarge biaxial strains in suspended monolayer MoS_2. Nano Lett, 2016, 16: 5836–5841
52 Yang J A, Bennett R K A, Hoang L, et al. Biaxial tensile strain enhances electron mobility of monolayer transition metal dichalcogenides. ACS Nano, 2024, 18: 18151–18159
53 Yu Y, Dong C D, Binder R, et al. Strain-induced indirect-to-direct bandgap transition, photoluminescence enhancement, and linewidth reduction in bilayer $MoTe_2$. ACS Nano, 2023, 17: 4230–4238
54 Island J O, Kuc A, Diependaal E H, et al. Precise and reversible band gap tuning in single-layer $MoSe_2$ by uniaxial strain. Nanoscale, 2016, 8: 2589–2593
55 Desai S B, Seol G, Kang J S, et al. Strain-induced indirect to direct bandgap transition in multilayer WSe_2. Nano Lett, 2014, 14: 4592–4597
56 Schmidt R, Niehues I, Schneider R, et al. Reversible uniaxial strain tuning in atomically thin WSe_2. 2D Mater, 2016, 3: 021011
57 Michail A, Anestopoulos D, Delikoukos N, et al. Tuning the Photoluminescence and Raman response of single-layer WS_2 crystals using biaxial strain. J Phys Chem C, 2023, 127: 3506–3515
58 Priyanka, Ritu, Kumar V, et al. Tailoring the electronic and optical properties of ReS_2 monolayer using strain engineering. Micro NanoStruct, 2024, 192: 207873
59 Ren H, Xiang G, Lu J, et al. Biaxial strain-mediated room temperature ferromagnetism of ReS_2 web buckles. Adv Elect Mater, 2019, 5: 1900814
60 Zhang G, Huang S, Chaves A, et al. Infrared fingerprints of few-layer black phosphorus. Nat Commun, 2017, 8: 14071
61 Huang S, Zhang G, Fan F, et al. Strain-tunable van der Waals interactions in few-layer black phosphorus. Nat Commun, 2019, 10: 2447
62 Wan J, Guo J, Hu F. Identification of strained black phosphorous by Raman spectroscopy. J Semicond, 2017, 38: 042003
63 Levitas V I, Kamrani M, Feng B. Tensorial stress-strain fields and large elastoplasticity as well as friction in diamond anvil cell up to 400 GPa. npj Comput Mater, 2019, 5: 94
64 Pei S, Zhang Z, Jiao C, et al. Quantitative regulation of electron-phonon coupling. Rep Prog Phys, 2024, 87: 078001
65 Dou X, Ding K, Jiang D, et al. Tuning and identification of interband transitions in monolayer and bilayer molybdenum disulfide using hydrostatic pressure. ACS Nano, 2014, 8: 7458–7464
66 Wen T, Zhang M, Li J, et al. Orientation-polarization dependence of pressure-induced Raman anomalies in anisotropic 2D ReS_2. Nanoscale Horiz, 2023, 8: 516–521
67 Sasaki T, Kondo K, Akahama Y, et al. Raman spectroscopy of two-dimensional material under high pressure: Black phosphorus ultrathin film, phosphorene. Jpn J Appl Phys, 2017, 56: 05FB06
68 Chi Z H, Zhao X M, Zhang H, et al. Pressure-induced metallization of molybdenum disulfide. Phys Rev Lett, 2014, 113: 036802
69 Zhang Z, Jiao C, Pei S, et al. Pressure-triggered stacking dependence of interlayer coupling in bilayer WS_2. Sci China-Phys Mech Astron, 2024, 67: 288211
70 Xie X, Ding J, Wu B, et al. Pressure-induced dynamic tuning of interlayer coupling in twisted WSe_2/WSe_2 homobilayers. Nano Lett, 2023, 23: 8833–8841
71 Rahman S, Saqib H, Liang X, et al. Pressure-induced metallization and robust superconductivity in pristine 1T-$HfSe_2$. Mater Today Phys, 2022, 25: 100698
72 Nayak A P, Pandey T, Voiry D, et al. Pressure-dependent optical and vibrational properties of monolayer molybdenum disulfide. Nano Lett, 2015, 15: 346–353
73 Martins L G P, Carvalho B R, Occhialini C A, et al. Electronic band tuning and multivalley Raman scattering in monolayer transition metal dichalcogenides at high pressures. ACS Nano, 2022, 16: 8064–8075
74 Li Y, Zhang X, Wang J, et al. Engineering interlayer electron-phonon coupling in WS_2/BN heterostructures. Nano Lett, 2022, 22: 2725–2733
75 Xia J, Li D, Zhou J, et al. Pressure-induced phase transition in Weyl semimetallic WTe_2. Small, 2017, 13: 1701887
76 Qi Y, Naumov P G, Ali M N, et al. Superconductivity in Weyl semimetal candidate $MoTe_2$. Nat Commun, 2016, 7: 11038
77 Zhao Z, Zhang H, Yuan H, et al. Pressure induced metallization with absence of structural transition in layered molybdenum diselenide. Nat Commun, 2015, 6: 7312
78 Clark S M, Jeon K J, Chen J Y, et al. Few-layer graphene under high pressure: Raman and X-ray diffraction studies. Solid State Commun, 2013, 154: 15–18
79 Nicolle J, Machon D, Poncharal P, et al. Pressure-mediated doping in graphene. Nano Lett, 2011, 11: 3564–3568
80 Mu L, Xing Q, Mou Y, et al. Highly tunable interlayer coupling and electronic structures of few-layer graphene with pressure. Nano Lett, 2024, 4c02035
81 Ni K, Du J, Yang J, et al. Stronger interlayer interactions contribute to faster hot carrier cooling of bilayer graphene under pressure. Phys Rev Lett, 2021, 126: 027402
82 Ke F, Chen Y, Yin K, et al. Large bandgap of pressurized trilayer graphene. Proc Natl Acad Sci USA, 2019, 116: 9186–9190
83 Hanfland M, Beister H, Syassen K. Graphite under pressure: equation of state and first-order Raman modes. Phys Rev B, 1989, 39: 12598–12603
84 Lu S, Yao M, Yang X, et al. High pressure transformation of graphene nanoplates: a Raman study. Chem Phys Lett, 2013, 585: 101–106
85 Cuscó R, Pellicer-Porres J, Edgar J H, et al. Pressure dependence of the interlayer and intralayer E_{2g} Raman-active modes of hexagonal BN up to the wurtzite phase transition. Phys Rev B, 2020, 102: 075206
86 Pei S, Wang Z, Xia J. High pressure studies of 2D materials and heterostructures: a review. Mater Des, 2022, 213: 110363
87 Tan S J R, Sarkar S, Zhao X, et al. Temperature- and phase-dependent phonon renormalization in 1T′-MoS_2. ACS Nano, 2018, 12: 5051–5058
88 Xia J, Wang J, Chao D, et al. Phase evolution of lithium intercalation dynamics in 2H-MoS_2. Nanoscale, 2017, 9: 7533–7540
89 Zulkefli A, Mukherjee B, Sahara R, et al. Enhanced selectivity in volatile organic compound gas sensors based on ReS_2-FETs under light-assisted and gate-bias tunable operation. ACS Appl Mater Interfaces, 2021, 13: 43030–43038
90 Zhong W, Zhang H, Karaca E, et al. Pressure-sensitive multiple superconducting phases and their structural origin in van der Waals HfS_2 up to 160 GPa. Phys Rev Lett, 2024, 133: 066001
91 Guan B, Ma F, Wu R, et al. Quantification of electron-phonon interaction in bismuth telluride under hydrostatic pressure via ultrafast spectroscopy. Appl Phys Lett, 2024, 125: 042201
92 Pan X C, Chen X, Liu H, et al. Pressure-driven dome-shaped superconductivity and electronic structural evolution in tungsten ditelluride. Nat Commun, 2015, 6: 7805
93 Ji C, Levitas V I, Zhu H, et al. Shear-induced phase transition of nanocrystalline hexagonal boron nitride to wurtzitic structure at room temperature and lower pressure. Proc Natl Acad Sci USA, 2012, 109: 19108–19112
94 Hromadová L, Martoňák R. Pressure-induced structural transitions in BN from ab initio metadynamics. Phys Rev B, 2011, 84: 224108
95 Kürkçü C, Yamçıçıer Ç. Structural, electronic, elastic and vibrational properties of two dimensional graphene-like BN under high pressure. Solid State Commun, 2019, 303: 113740
96 Gong L, Kinloch I A, Young R J, et al. Interfacial stress transfer in a graphene monolayer nanocomposite. Adv Mater, 2010, 22: 2694–2697
97 Liu Z, Amani M, Najmaei S, et al. Strain and structure heterogeneity in MoS_2 atomic layers grown by chemical vapour deposition. Nat Commun, 2014, 5: 5246
98 Lee C, Wei X, Kysar J W, et al. Measurement of the elastic properties and intrinsic strength of monolayer graphene. Science, 2008, 321: 385–388

99 Yang J C, Lee S, Ma B S, et al. Geometrically engineered rigid island array for stretchable electronics capable of withstanding various deformation modes. Sci Adv, 2022, 8: eabn3863
100 Zhang L, Marcus C, Lin D, et al. A conformable phased-array ultrasound patch for bladder volume monitoring. Nat Electron, 2023, 7: 77–90
101 Liu X, Wang Q, Zhou S, et al. Stiffness and interface engineered soft electronics with large-scale robust deformability. Adv Mater, 2024, 36: 2407886
102 Wang Y K, Ge M, Tan J N, et al. Dipole-moment modulation of photovoltaic and photoresponse properties in 2H-MoSSe/MoS_2 van der Waals heterojunctions under electric field. Sci China Inf Sci, 2025, 68: 159402
103 Liu X, Fu Q, Liao H, et al. Direct linearly polarized emission in van der Waals LEDs via flexoelectric effect. Laser Photon Rev, 2025, 19: 2401319
104 Novoselov K S, Mishchenko A, Carvalho A, et al. 2D materials and van der Waals heterostructures. Science, 2016, 353: aac9439
105 Liu A, Zhang X, Liu Z, et al. The roadmap of 2D materials and devices toward chips. Nano-Micro Lett, 2024, 16: 119
106 Katiyar A K, Hoang A T, Xu D, et al. 2D materials in flexible electronics: recent advances and future prospectives. Chem Rev, 2024, 124: 318–419
107 Luo Y, Abidian M R, Ahn J H, et al. Technology roadmap for flexible sensors. ACS Nano, 2023, 17: 5211–5295
108 Finneran I A, Welsch R, Allodi M A, et al. Coherent two-dimensional terahertz-terahertz-Raman spectroscopy. Proc Natl Acad Sci USA, 2016, 113: 6857–6861
109 Venanzi T, Cuccu M, Perea-Causin R, et al. Ultrafast switching of trions in 2D materials by terahertz photons. Nat Photon, 2024, 18: 1344–1349
110 Jin W, Kim H H, Ye Z, et al. Raman fingerprint of two terahertz spin wave branches in a two-dimensional honeycomb Ising ferromagnet. Nat Commun, 2018, 9: 5122
111 Zhu J, Xu B, Xiao F, et al. Frequency scaling, elastic transition, and broad-range frequency tuning in WSe_2 nanomechanical resonators. Nano Lett, 2022, 22: 5107–5113
112 Xu B, Zhang P, Zhu J, et al. Nanomechanical resonators: toward atomic scale. ACS Nano, 2022, 16: 15545–15585
113 Zhang X, Makles K, Colombier L, et al. Dynamically-enhanced strain in atomically thin resonators. Nat Commun, 2020, 11: 5526
114 Tang J, Su Z L, Cai S, et al. HF-VHF NEMS resonators enabled by 2D semiconductor $ReSe_2$. Sci China Inf Sci, 2024, 67: 209401
115 Xu B, Zhang Z, Qin J, et al. Dynamic tuning of terahertz atomic lattice vibration via cross-scale mode coupling to nanomechanical resonance in WSe_2 membranes. Microsyst Nanoeng, 2025, 11: 18
116 Hu K, Liu R, Liu S, et al. A rapid compression large-volume press with a high pressure jump above 10 GPa within milliseconds. Rev Sci Instruments, 2024, 95: 103905
117 Feng B, Xie L, Hou X, et al. A virtual thermometer for ultrahigh-temperature-pressure experiments in a large-volume press. Matter Radiat at Extremes, 2024, 9: 047401
118 Shang Y C, Shen F R, Hou X Y, et al. Pressure generation above 35GPa in a walker-type large-volume press*. Chin Phys Lett, 2020, 37: 080701